Development and field tests of GEM, the Ocean's Kite: A submersible floating device to tap tidal current energy

This paper presents the results of a series of test campaigns performed on an innovative system to harness clean energy from marine and river currents, developed in cooperation with the University of Naples "Federico II". It consists of an underwater vehicle linked to the seabed by means of a tether and supporting two hydro-turbines. Preliminary studies and experimental results of wind tunnel and towing tank tests on both single turbine and a complete scaled model will be illustrated. The behavior and performances of different configurations in both nominal and off-design conditions will be highlighted. Finally experimental results on a full-scale prototype installed in the Venetian lagoon will be presented.

DOI: 10.12910/EAI2015-038

D.P. Coiro, G. Troise, F. Scherillo, N. Bizzarrini, G. Calise

Introduction

The exploitation of marine and river current power over the last few years has become one of the most promising fields in energy production from renewable sources, thanks to their low environmental impact and more stable and predictable behaviour with respect to other sources.

The ADAG (Aircraft Design & Aero Flight Dynamics) research group, in cooperation with Dr. Nicola Giorgio Morrone and Seapower Scarl, has developed since 2005 [1, 2] a system named GEM, The Ocean's Kite, specifically suited for this kind of energy sources. It is suitable for applications in both oceans and rivers. A CAD drawing of GEM is shown in Figure 1.

FIGURE 1 GEM, concept CAD drawing

It consists of a tethered system employing two shrouded, horizontal-axis turbines, mounted on both sides of two central floating bodies.

The upper body is designed to provide the necessary buoyancy force, while the lower one is used as dead weight. The upper body is

Contact person: Domenico P. Coiro
coiro@unina.it

also equipped with a "V-tail" to augment the longitudinal and lateral stability of the whole system and to allow the regulation of the pitching attitude into the stream by means of an adjustable flap. The tail also serves as damping device of lateral-directional oscillations. The two hydrokinetic turbines are counter-rotating and equipped with a diffuser (eventually with leading edge slats to enhance their aerodynamic role of accelerating the local velocity field toward the turbine rotor disks) to reduce the dimensions of actuator disks for a given rated power.
The system has a winch to allow the emersion of the system for control and maintenance purposes. A control system specifically designed avoids the rotation of GEM over 360 degrees and the twisting of the electrical cable.
The GEM has been designed to have specific advantages in terms of constructive simplicity and ease of operation, a relatively safe and easy self-orienting behaviour but, first of all, the possibility of avoiding the use of expensive submarine foundations, replaced by an anchorage to a single point on the seabed with a flexible tethering cable.
Two scaled models have been tested in the towing tank of the Department of Industrial Engineering (DII) at the University of Naples and a full-scale prototype has been tested in an open sea site, in order to characterize the static and dynamic behaviour of the system.
The present work will show a summary of the towing tank tests on a scaled model of the system and a brief report of the main results of the full-scale prototype testing in real sea conditions. Results of a simple numerical model of the GEM system equilibrium will also be discussed. The numerical model has been validated by comparing the results with experimental data.

Towing tank experimental tests

Characterization of the system and tests setup

The behaviour of the whole system was analysed under steady state and dynamic conditions in the DIN towing tank shown in Figure 2.

FIGURE 2 DII towing tank

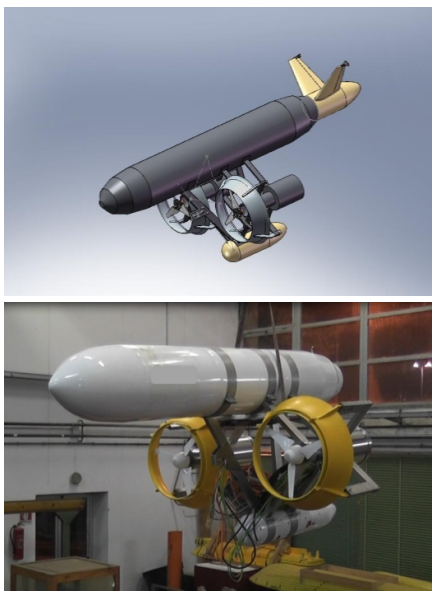

FIGURE 3 GEM prototype for towing tank tests. Scale 1:8

Turbine diameters	0.61 m
Distance between turbine axes	1.13 m
GEM overall length	3.55 m
GEM overall height	1.84 m

TABLE 1 GEM model. Main geometric data

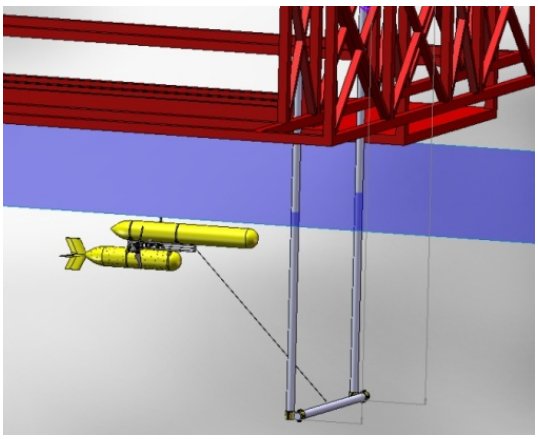

FIGURE 4 GEM model. Schematic of the testing support structure

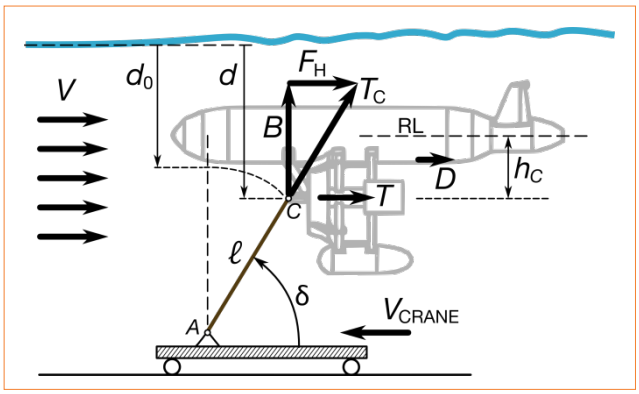

FIGURE 5 Schematic of the GEM system in a steady-state condition, immersed in a flow current

Initial depth d_0 of attachment point C	1.65 m
Depth d_A of towing attachment point A	3.27 m
Distance h_C of attachment point C from upper body reference line (RL)	0.75 m
Cable length, ℓ	1.62 m

TABLE 2 Geometric data of GEM model tethering system

Both nominal and off-design conditions were investigated by using differential braking of the two turbines. Off-design conditions may be caused in real conditions, for example, by an abnormal setback of one turbine.

The DII towing tank is 120 m long, 10 m wide and 5 m deep. A travelling crane carries the model at the desired velocity and a wave generator can simulate different operating conditions.

The actual shape of the model tested is shown in Figure 3, and the main dimensions are reported in Table 1.

Two electrical asynchronous motors (controlled by two inverters) acted on the turbine axes to control the rotational speed. Each of the two turbines was controlled separately.

The system was cable-connected to a steel frame structure attached to the travelling crane, as shown in Figure 4, and was then submerged in the tank at the desired depth by releasing, or tightening, the tether through a winch.

A schematic of the GEM system in a steady-state condition, immersed in a flow current, is shown in Figure 5. The equilibrium involves the cable tension force T_C, the buoyancy B, and the total horizontal force F_H. A list of geometric data of the GEM model tethering system is reported in Table 2.

The thrust T of the two ducted turbines (see Fig. 5) contribute to F_H as well as the hydrodynamic drag D of the submerged body. The combination of F_H and the buoyancy B is counter-balanced by the cable traction T_C.

The quantities observed and measured during the tests include:

- the attitude in terms of acceleration, velocity and angular displacement of the GEM by using an inertial platform located on board the floating body;
- the traction (Tc) on the tether cable by means of a dedicated load cell;
- torque and angular velocity of the left-hand-side turbine, from which the output power can be estimated (assuming symmetrical operating conditions) using a torquemeter;
- rotor and diffuser thrust with load cells.

The power is evaluated as $P=Q\Omega$, i.e. the torque times the angular speed.

Tests have been performed at various rotational speeds

and placing the model at various depths. In the following we consider the coefficient of power (or efficiency) defined as

$$C_P = \frac{P}{\frac{1}{2}\rho V^3 A} \qquad (1)$$

where P is the output measured power (left-hand-side turbine), V is the velocity of the current (i.e. the steady-state crane speed), A is the area of a reference surface (coincident with the turbine disk area), and ρ is the water density. Similarly, we define the torque coefficient as

$$C_Q = \frac{Q}{\frac{1}{2}\rho V^2 AR} \qquad (2)$$

where Q is the torque at the turbine hub and R is the nominal turbine disk radius. The thrust coefficient of the single turbine C_T is defined as

$$C_T = \frac{T}{\frac{1}{2}\rho V^2 A} \qquad (3)$$

where T is the thrust on turbine. The thrust (or drag) coefficient of the whole system is defined as

$$C_D = \frac{F_H}{\frac{1}{2}\rho V^2 S_{ref}} \qquad (4)$$

where F_H is the total drag (a horizontal force) developed by the system and S_{ref} is a reference area (not necessarily equal to A). Finally, the tip speed ratio is defined as

$$TSR = \frac{\Omega R}{V} \qquad (4a)$$

where Ω is the turbine angular speed. The TSR is a non-dimensional measure of the rotor tip speed.

Experimental results

Turbine Efficiency

Two test campaigns have been carried out: the first related to a single turbine with and without the shroud, and the other related to the whole system-scaled prototype. The main result of the experimental tests is the comparison of C_P and C_Q versus TSR between GEM configurations with bare and shrouded turbines.

The main aim of using a shroud is to improve the turbine efficiency. Its function is to increase the mass flow rate through the turbine disc with a consequent power augmentation. The shroud had been previously optimised with a simple design method [3] and the experimental results have been confirmed by a CFD analysis.

As shown by [3,4,5] the power augmentation is proportional to the thrust exerted by the flow on the diffuser. The shroud design criteria were based on the maximization of this thrust, which is related to the chord, angle of attack, and lift coefficient of the diffuser airfoil section.

A high-lift airfoil has been opportunely chosen and a simple design method carried out [3] in order to define an optimum diffuser pitch angle and, consequently, its working angle of attack.

This simple design procedure is subject to several approximations: viscous effects are neglected, the induction factor is evaluated to be constant along the turbine radius, the shroud equivalent diameter d is approximated to the turbine diameter. In order to

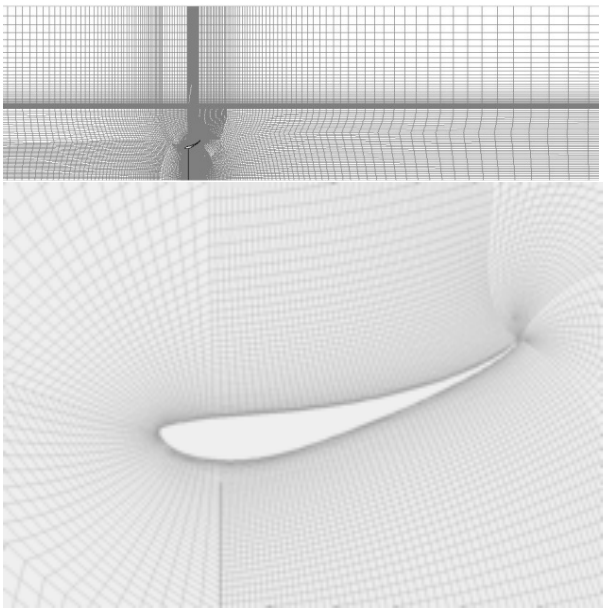

FIGURE 6 Mesh domain

evaluate the design diffuser angle more accurately, a numerical simulation has been carried out using FLUENT.

The turbine has been simulated as a constant pressure jump across the flow. The viscous effect has been included and the realizable k-ε turbulence model with enhanced wall treatment was used. Due to the axial symmetry of the system around the turbine axis a two-dimensional mesh has been created applying the axisymmetric solution option, see Figure 6. The maximum C_P is reached for a pitch value (i.e., the angle that diffuser airfoil section makes with axial direction) of ~ 26°.

Using the results obtained by the numerical simulation experimental tests were carried out both in wind tunnel and in the towing tank on an isolated turbine in order to characterize its effective behaviour. Figure 7 reports the comparison of power coefficient for the bare turbine, a 23° shrouded turbine and a 26° shrouded turbine obtained during the wind tunnel tests.

The geometry with 26° section pitch has shown a better performance and has been chosen for further development. During towing tank tests different TSR values were obtained by using varying rotation speeds of the turbines and a fixed crane speed $V = 1.5\ m \cdot s^{-1}$. In Figure 8 a typical time history of the controlled angular speed of the turbines, crane speed V and torque Q measured at the turbine hub have been reported. This

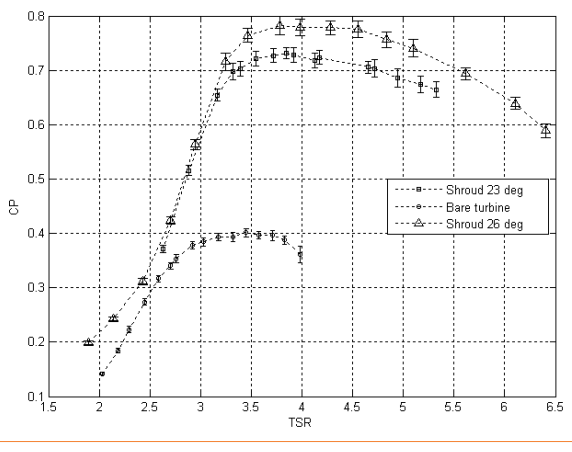

FIGURE 7 Comparison of C_P (*TSR*) for bare turbine, 23° shrouded turbine and 26° shrouded turbine. Wind tunnel tests

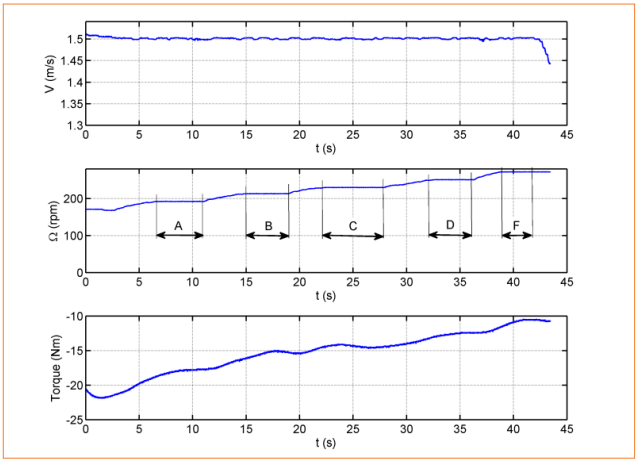

FIGURE 8 Time histories of crane advance speed, turbine controlled angular speed, and torque (turbines with diffusers, upright V-tail)

is the torque applied by the motor in order to obtain the desired TSR.

The time intervals named "A", "B", "C", "D", and "F" correspond to constant angular speed that means constant TSR. Details of the testing structure and load cells are shown in figures 9, 10 and 11.

In Figure 12 we report the experimental power coefficient curves for an isolated turbine versus *TSR*, tested in water both with and without diffuser.

The curves confirm wind tunnel results and show the advantage of using ducted turbines that results in almost a doubling of the maximum efficiency $C_{P,max}$.

It is worth noting that the power coefficient of the shrouded configuration is referred to the rotor disk surface area and that referring it to the overall frontal area (equal to the exit area of the shroud) the net increase is reduced at about 7%, as shown in Figure 13.

The yaw angle influence was also analyzed. Comparison between maximum *Cp* value versus yaw angle for ducted and non-ducted case is reported in Figure 14.

The maximum power coefficient of the bare turbine decreases linearly with the yaw angle, whereas the shrouded turbine seems to be not influenced by the yaw angle between 0 and 10 deg.

Experimental power coefficients for the turbines tested with the whole system confirm results for isolated turbines. The curves are reported in Figure

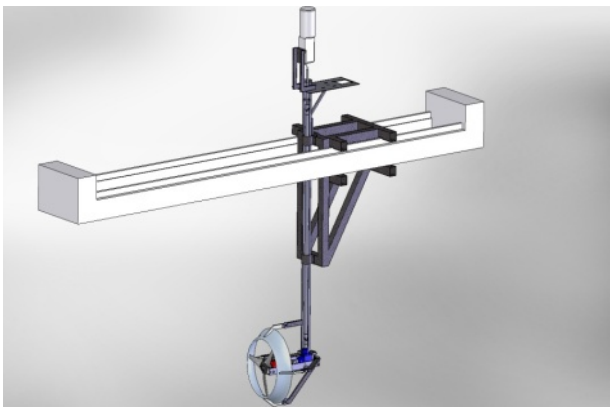

FIGURE 9 CAD view of the testing structure for an isolated turbine

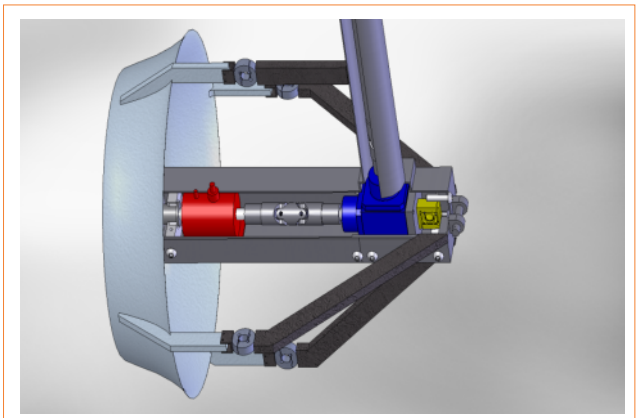

FIGURE 10 Detail of the diffuser on the support structure

FIGURE 11 Real testing structure

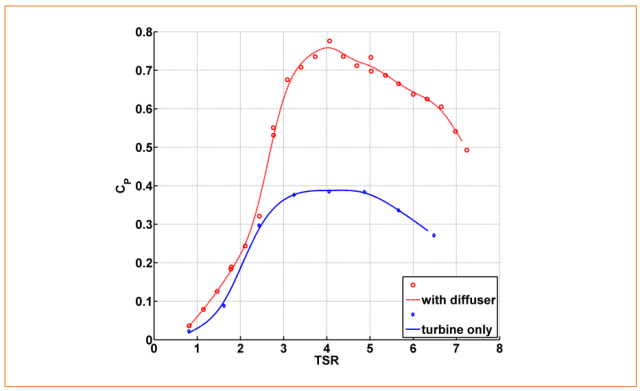

FIGURE 12 Comparison between bare and shrouded turbine. Single turbine test

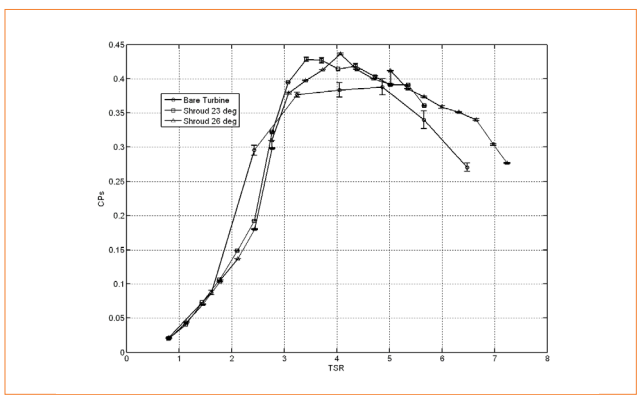

FIGURE 13 Towing tank tests: Comparison referring the coefficient to the diffusers exit areas

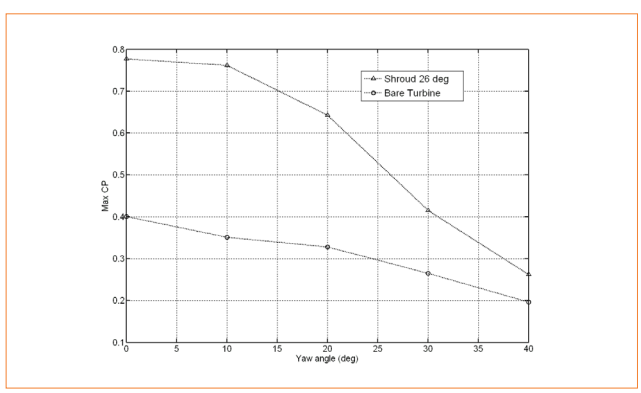

FIGURE 14 Maximum CP versus yaw angle comparison

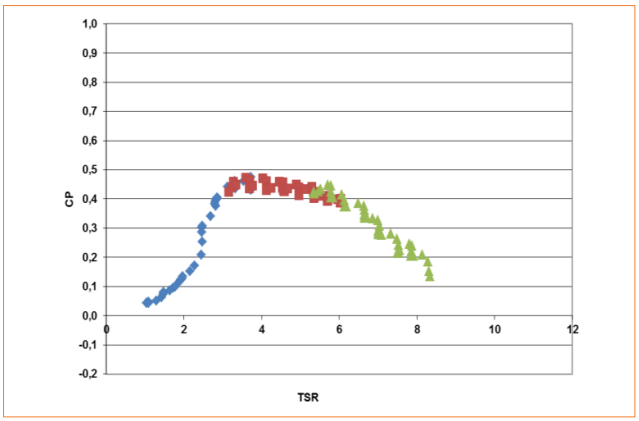

FIGURE 15 Experimental power coefficient values (turbines without diffusers, upright V-tail, V = 1.5 m·s-1)

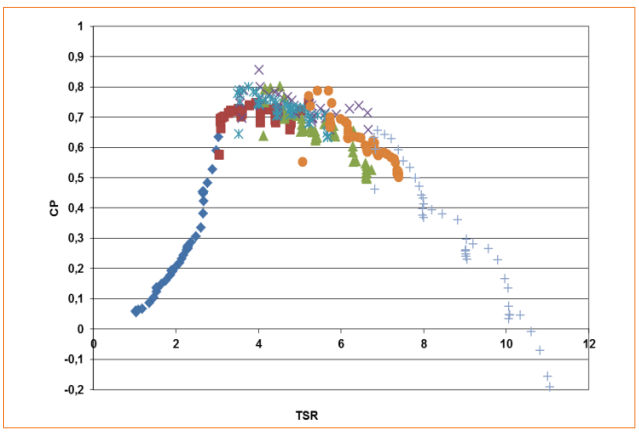

FIGURE 16 Experimental power coefficient values (turbines with diffusers, upright V-tail, V = 1.5 m·s^{-1})

	CP,max	*TSR @ CP,max*
Ducted turbines	0.74	4.1
Turbines w/o diffusers	0.40	4.0

TABLE 3 GEM efficiencies with and without diffusers

15 and Figure 16 for both the ducted and bare turbines cases and maximum *Cp* with relative *TSR* is reported in Table 3.
The fitting curve of power coefficient versus *TSR* is shown in Figure 17.

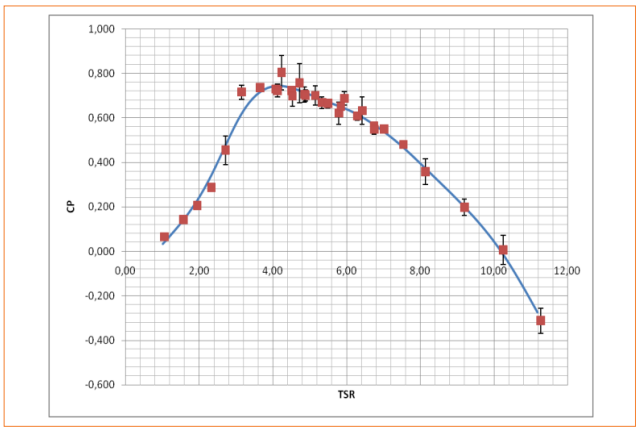

FIGURE 17 Power coefficient (turbines with diffusers, upright V-tail, V = 1.5 m·s-1)

Starting torque

The start-up torque Q_0 is the minimum torque needed to put the turbines in rotation in a current of given speed V. It is related to the minimum current speed above which the system is capable of generating power.
To assess Q_0 the turbine has been towed at different speeds keeping a zero angular speed by using a control motor. The measured torque acting in this case is identified with the required start-up torque Q_0 at the corresponding current speed V. The measured Q_0 and the corresponding torque coefficient C_{Q_0} at different current speeds are reported in Table 4 and Q_0 is shown in Figure 18. By averaging the values of Q_0 we have obtained the curve in Figure 19.

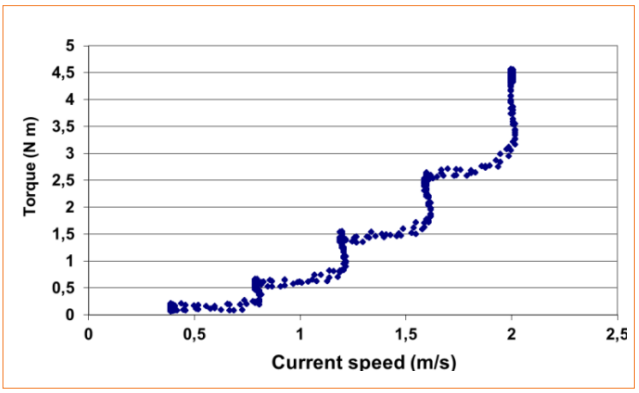

FIGURE 18 Measured start-up torque Q_0 at different current speeds (and zero angular speed)

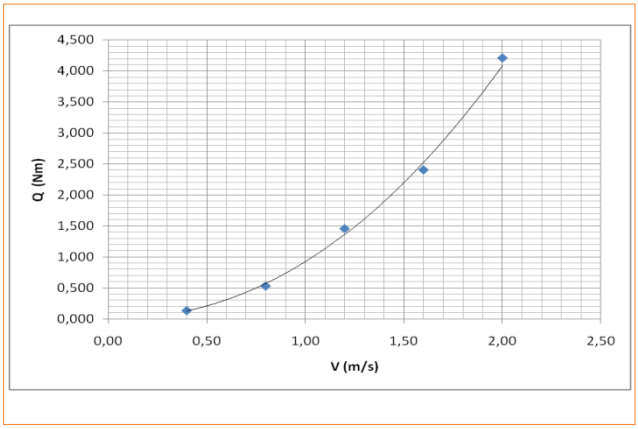

FIGURE 19 Variation of turbine start-up torque with current speed

V (m·s⁻¹)	C_{Q_0}	Q_0 (N·m)
0.40	0.0180	0.132
0.80	0.0181	0.528
1.20	0.0221	1.455
1.60	0.0205	2.403
2.00	0.0230	4.210

TABLE 4 GEM turbine measured start-up torques

Turbine thrust

In Figure 20 thrust coefficient C_T versus *TSR* is illustrated

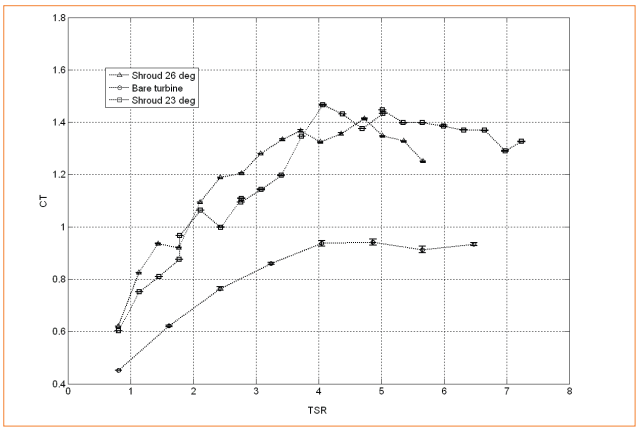

FIGURE 20 Turbine thrust coefficient comparison (coefficient referred to the turbine area)

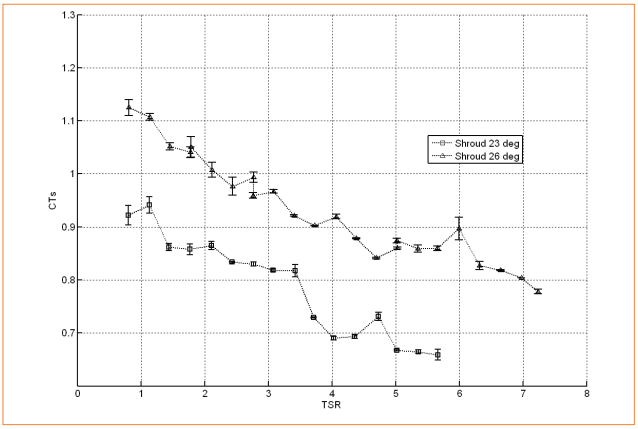

FIGURE 21 Shroud thrust coefficient comparison (coefficient referred to the turbine area)

for the bare turbine and for two diffusers with the same section but two different incidence angles (23° and 26°).
In discordance to some theories about the diffuser working principles, the diffuser causes a sensible increase in thrust coefficient on the rotor. Such results need further investigations and validations.
In Figure 21 shroud thrust coefficient C_T versus *TSR* is reported. The reduction with increasing *TSR* may be related to a reattachment of the flow over the diffuser inner side, due to the interaction with the turbine-induced flow.

Tether tension and inclination

Another important feature being investigated during the experimental tests is the amount of tension in the cable connecting the GEM to the crane. This gives an idea of the maximum stress to be accounted for when dimensioning the cable of the real system and enables the appropriate selection of the mooring and anchorage system. A load cell was used to observe the tether cable force T_C.
Considering the scheme of Figure 5, we derived two formulae for calculating the tether angle δ and the total horizontal force F_H. The amount of the buoyancy, i.e. the intensity of B, is observable in static conditions. Knowing B and by measuring T_c, we can calculate F_H and δ by the expressions:

$$\delta = \frac{\pi}{2} - \cos^{-1}\left(B / T_C\right) \qquad (5)$$

(6)

Measures of δ and F_H versus the angular speed Ω, for a constant current speed V=1.5 m·s^{-1} are reported in Figure 23 and 24.

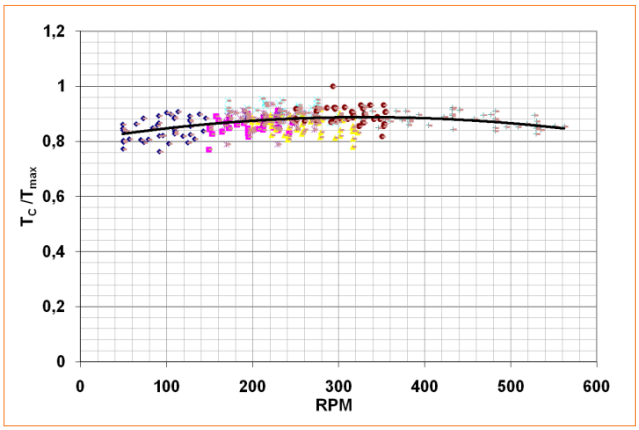

FIGURE 22 Tension force at the connection tether, referred to the maximum tension observed (turbines with diffusers, upright V-tail, V = 1.5 m·s-1)

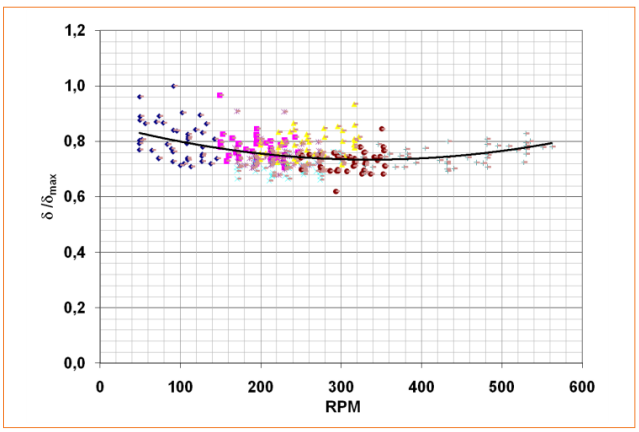

FIGURE 23 Measured tether angle with respect to the horizontal plane (turbines with diffusers, upright V-tail, V = 1.5 m·s-1)

Figure 25 shows the steady-state tether angle versus current speed V as calculated by observing the underwater vertical displacement d of the floating body during the tests. Knowing the cable length ℓ and the initial

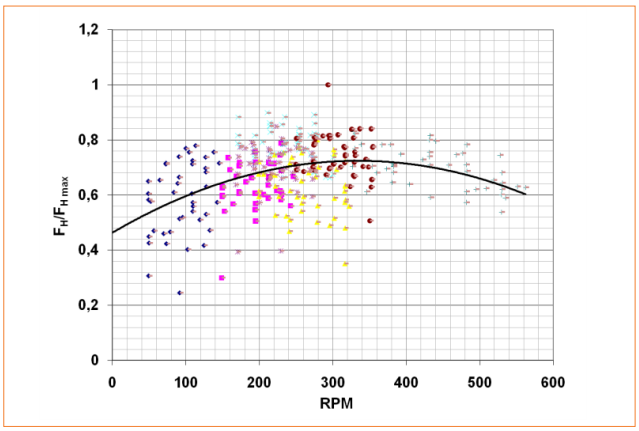

FIGURE 24 Resistance to the advancement motion opposed by the GEM, referred to the maximum value observed (turbines with diffusers, upright V-tail, V = 1.5 m·s-1)

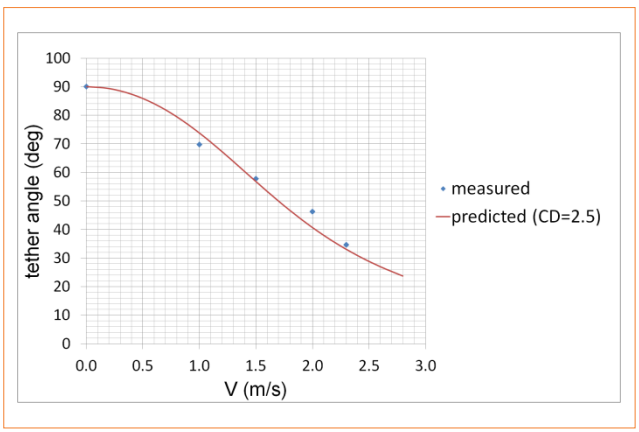

FIGURE 25 Steady-state tether angle (turbines with diffusers, upright V-tail). The solid line is predicted with a simplified model assuming a constant *CD*

static displacement d_0 (when V = 0), and observing the actual depth d, the angle δ may be calculated.
The solid line is predicted with a simplified model, assuming a constant total drag coefficient.

Full-scale prototype tests

Prototype general data

A full-scale prototype of a GEM system, shown in Figure

FIGURE 26 GEM full-scale prototype

Turbine diameter:	D_t=3.08 m
Diffuser throat diameter:	D_g=3.10 m
Diffuser exit area diameter:	D_e=4.08 m

TABLE 5 Turbine and diffuser dimensions

Overall length:	L=9.2 m
Overall height:	H=5.2 m
Overall width:	S=10.4 m

TABLE 6 Floating support structure dimensions

Overall weight:	W = 16100 kg
Net buoyancy force:	B = 51000 N
Horizontal thrust (on the overall system at 1.5 m·s^{-1}):	T = 45000 N
Rotational speed:	Ω = 38 RPM

TABLE 7 Weight, loads and operational characteristics

Depth (range): 15 m to 9.8 m (without current)
Nominal power 20 kW with a tidal current of 1.5 m·s^{-1}
Three-blades 3 m diameter rotor
Innovating blade section profiles
Carbon blades - Fiberglass diffuser
Rotor Efficiency: 0.8

TABLE 8 Technical and operational data

26, dimensioned to produce 20 kW at current speed of 1.5 m·s^{-1}, has been developed, built and installed in a test site. It has been partially sponsored by a consortium of companies operating in the Veneto region and partially by the Veneto Regional Authority.
The first prototype has been deployed in the Venice lagoon, near Forte Sant'Andrea, with a seabed depth of about 25 m. The system was operating at a depth of about 15 m.
In the Tables 5, 6, 7 and 8 overall dimensions of the prototype are reported.
On the basis of the preliminary development phase and the results of the towing tank tests, some of the operational and load data reported in Table 7 and Table 8 have been estimated for the prototype.

Measurement equipment

The following equipment has been installed on board the system:

- Inclinometer:
  - pitch angle,
  - roll angle;
- Pressure sensors:
  - depth;
  - Generators related data:
  - actual power,
  - actual torque,
  - actual number of revolutions of the engine,
  - torque and speed imposed by the controller;
- Wind vane on the floating body:
  - water current relative direction.

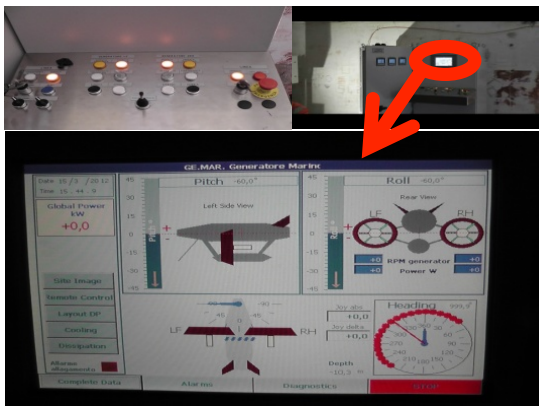

FIGURE 27 Data acquisition system software overview

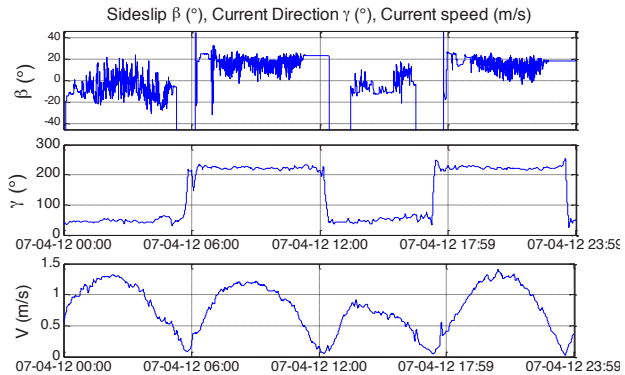

FIGURE 28 Typical time histories of current velocity direction (γ) and magnitude (*V*) during one-day observation. Current relative direction with respect to the system longitudinal axis is also reported (sideslip β). Current direction (γ) represents the direction of the flow velocity with respect to the north

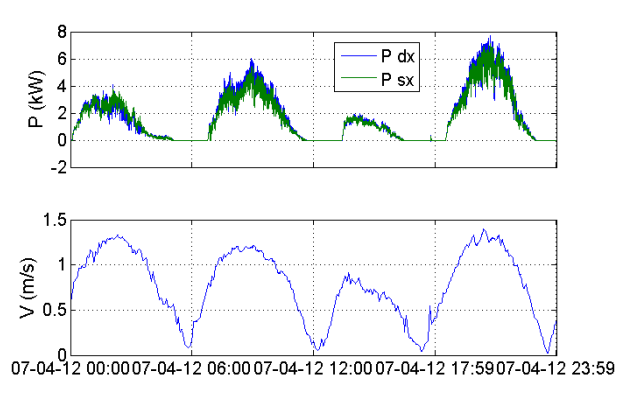

FIGURE 29 Generator power production of left and right turbines and current speed variation during the tide

The data have been recorded on board and radio-transmitted to a remote server. An acoustic speed sensor (ADCP) has been installed in proximity of the GEM to reconstruct the current velocity profile for the whole depth range. Typical measured data are reported in Figure 28.
Figure 28 shows a typical reversing pattern, characteristic of tidal current, while Figure 29 shows both produced electrical power and current speed during the day.

Experimental results

The power was measured for both the GEM turbines and is reported as a function of the measured speed in Figure 30. In order to better analyze the power performance, a binning procedure has been used (data are grouped in velocity bins over which an arithmetic mean is performed). The power curves for the right turbine after binning procedure and estimated shaft power are reported in Figure 31. As a reference, theoretical cubic power curves are also reported for a fixed power coefficient.

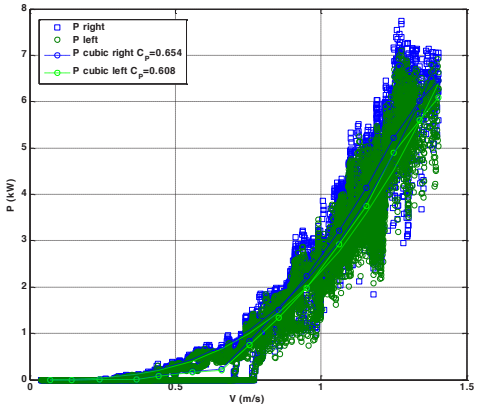

FIGURE 30 Left and right turbine power curve (best incoming direction)

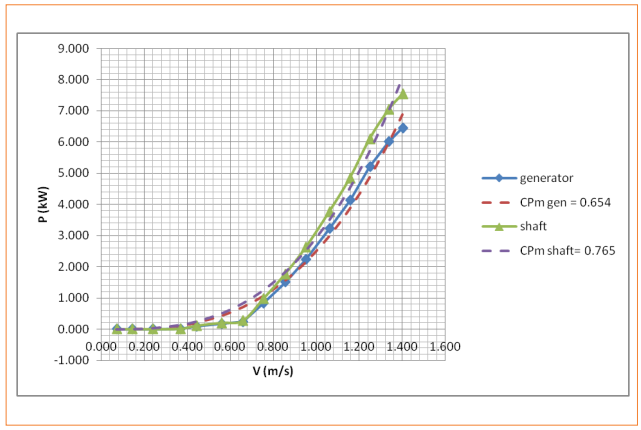

FIGURE 31 Power curve using binning technique. Right turbine. Electrical measured power compared to numerical estimated shaft power

Depth (range): 15 m to 9.8 m (without current)
Nominal power 100 kW with a tidal current of 2.6 m·s^{-1}
Three-blades 3 m diameter rotor
Innovating blade section profiles
Carbon blades - Fiberglass diffuser
Rated rotation speed: 65 rpm
Rotor Efficiency: 0.8
Expected average yearly production with 2.5 m·s^{-1} maximum
speed site: ~ 300 MWh

TABLE 9 Performance and technical data

The power coefficient may be estimated from the electrical measured power and has a value in the range $C_{P,max}$ = 0.6–0.65. Assuming an efficiency of the generator of 0.9 and a gearing efficiency of 0.9, a rough estimation of the shaft power coefficient may be obtained in the range $C_{P,max}$ = 0.75–0.8, which is in good agreement with previous model testing.
It has to be noted that the values of the power coefficient apparently exceed the Betz limit but this is obviously due to the presence of the diffuser. For details on Betz limit and diffuser augmented power coefficient, see for example [7]. To give an idea of the potential of a prototype of the same dimension deployed in a more energetic site, in Table 9 a list of characteristics for a prototype of a rated power of 100 kW at current speed of 2.6 m s^{-1} is reported.
Finally, inclinometers have been used to estimate the roll and pitch angle of the system that shows a relatively small oscillation around the levelled position, as expected for symmetry of the system.

Conclusions

Results of test campaigns of GEM model components in both wind tunnel and towing tank, small-scale model in towing tank and full-scale prototype in a real sea site have been presented and discussed. The advantages of using shrouded turbines have been shown since the power coefficient doubles its value relative to bare turbine. Both model and full-scale prototypes have also shown static and dynamic stability and good performances also in yawed flow condition.
The GEM system can represent a real breakthrough in the field of harnessing marine current energy thanks to its characteristics of easy deployment, no visual impact, reduced maintenance and operational costs as well as high performance, as proven in the present paper.

Acknowledgments
GEM has been patented by Dr. Nicola Giorgio Morrone and Prof. Domenico Coiro

Domenico P. Coiro, Nadia Bizzarrini, Giuseppe Calise
University of Naples "Federico II", Department of Industrial Engineering – Aerospace Division, Italy

Giancarlo Troise, Ferdinando Scherillo
SEAPOWER Scarl, consortium with University of Naples "Federico II", Italy

references

[1] D.P. Coiro, Development of Innovative Tidal Current Energy Converters: From Research to Deployment, Asian Wave and Tidal Energy Conference (AWTEC 2012), Jeju, South Corea, June 2012.

[2] D.P. Coiro, G. Troise, F.Scherillo, Design, towing tank test and deployment of full scale GEM, a novel tethered system for harnessing tidal energy, Asian Wave and Tidal Energy Conference (AWTEC 2012), Jeju, South Corea, June 2012.

[3] F. Scherillo, U. Maisto, G. Troise, D.P. Coiro, S. Miranda, Numerical and Experimental Analysis of a Shrouded Hydroturbine, Clean Electrical Power International Conference (ICCEP), 14-16 June 2011.

[4] S. Mertens, Wind turbine in the built environment, in *Multi Science*, p. 99, Essex, 2006.

[5] O. De Vries, Fluid dynamic aspects of wind energy conversion AGARDograph No. 243 NLR.

[6] R. Tognaccini, Lezioni di Aerodinamica dell'ala rotante Lectures notes, Università degli studi di Napoli Federico II, 2008.

[7] G.J.W. van Bussel, The science of making more torque from wind: Diffuser experiments and theory revisited, in *Journal of Physics: Conference Series*, 75, 2007.